International Journal of Emerging Technologies in Engineering Research (IJETER)
Volume 4, Issue 3, March (2016) www.ijeter.everscience.org

Power Loss Analysis of Single Switch Isolated Dc-Dc Converter Using ZVS and ZCS Techniques

M.Meenakhi
P.G Scholar, Dept. Of Electrical and Electronics Engineering, Gnanamani College of Engineering, Namakkal, India.

R.Gandhi
HOD, Department of Electrical and Electronics Engineering, Gnanamani College of Engineering, Namakkal, India.

R.Siva Kumar
Lecturer, Dept. Of Electrical and Electronics Engineering, Kongunadu Polytechnic College, Tiruchirapalli, India.

Abstract – This paper focuses on power loss analysis of single switch isolated DC-DC boost converter using quasi resonant ZVS (zero voltage switching) and ZCS(zero current switching). Low rated lossless snubber with low magnetizing current, 100kHz, 250W prototype converter are provided to validate the proposed concept. This design has high efficiency and low switching loss. The design and performance are verified through simulation using MATLAB environment.

Index Terms – Soft switching, Isolated Boost converter, Single switch.

1. INTRODUCTION

The proposed system is a combination of flyback and forward converters. Isolated dc-dc converters contains one main switch and one clamp switch creates ZVS and ZCS. ZVS reduces turn on switching loss and ZCS reduces turn of switching losses. Conventional PWM converters are operated under hard switching conditions, where rectangular voltages and currents of semiconductor devices are changed abruptly from high values to zero and vice versa at turn-on and turn-off, causing switching losses(Fig.2) and generating a substantial amount of electromagnetic interference.

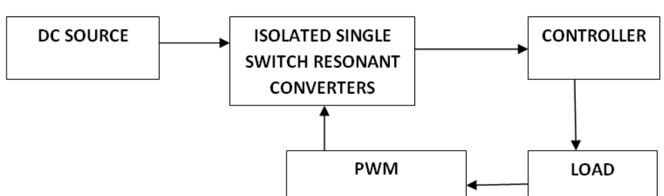

Fig.1. General Block diagram of Isolated DC-DC boost converter.

Since switching losses are proportional to the switching frequency fs , they limit the maximum switching frequency. A high level of EMI is due to a wide spectrum of harmonics contained in rectangular PWM waveforms. In addition, high current spikes caused by diode reverse recovery generate a large spectrum of harmonics. Switching losses and EMI level in dc–dc power converters can be reduced by soft switching techniques. Since semiconductor devices turn on or turn off at zero voltage or zero current, the product of the device voltage and current during the transitions is zero, eliminating switching losses. This allows for high switching frequencies, reducing the size and weight of the soft-switching converters due to lower values of reactive components. The harmonic content of the current and voltage waveforms is also reduced, yielding a lower level of EMI. Topologies of soft-switching converters absorb many parasitic components, such as transistor output capacitance, diode capacitance, and transformer leakage inductance. In the ZVS technique, a semiconductor device turns on at zero voltage. In the ZCS technique, a semiconductor device turns off at zero current.

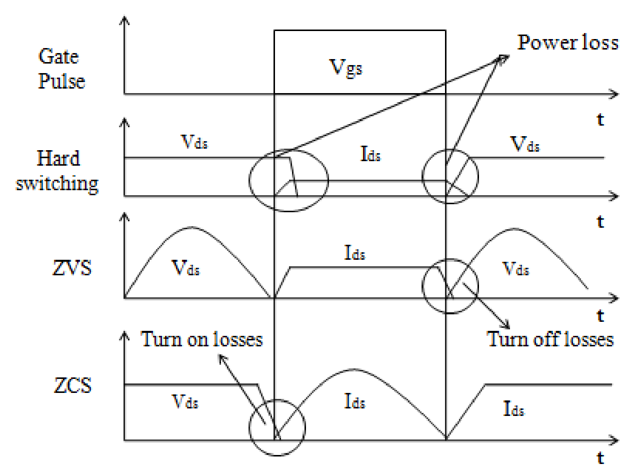

Fig .2 Effects of hard switching.

An isolated transformer is used to eliminate any direct electrical connection between the input and the output of the converter power stage. Since the operating frequency of PWM converters is much higher than 50–60Hz line frequency, the transformer, Inductors, and capacitors are much smaller than those operated at line frequencies.

2. PROPOSED SYSTEM

A.Open Loop Isolated Boost Converter with Single Switch

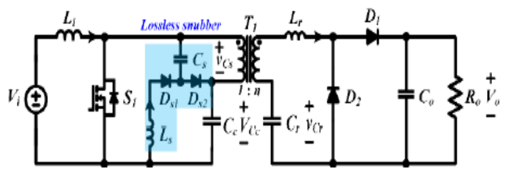

The value of the duty ratio is calculated using equation (1).

$$Vo = \frac{Vs}{1-D} \quad (1)$$

$$L = \frac{V_S D}{\Delta I_L fs} \quad (2)$$

$$C = \frac{D}{R\left(\frac{\Delta Vo}{Vo}\right) fs} \quad (3)$$

The values for the capacitance and inductance used for the simulations are calculated using equation (2) and (3),

For non-ideal case,

$$P_I = P_o + P_{Loss} \quad (4)$$

$$P_{Loss} = P_L + P_{sw} + P_D \quad (5)$$

P_{sw} ⟶ Total switching loss.

P_L ⟶ Inductance loss.

P_I ⟶ Input power.

$$P_{SW\,(LOSS)} = \frac{(V_0 * I_0 * f_s)}{2}(t_{on} + t_{off}) \quad (6)$$

$$P_L = r_L\, I_L^{\,2} \quad (7)$$

$$P_D = (1-D)V_D I_L \quad (8)$$

Output voltage calculated for non-ideal case Using equation (9).

$$VsIs = VoIo + r_L\, I_L^{\,2} + D_{rsw} I_L^{\,2} + \left(\frac{1}{2}\right)(C_{SW} V_0^{\,2} fs) + (1-D)V_D I_L$$

From the above equation we get,

$$Vo = \frac{VsR(1-D) - V_D R(1-D)^2}{R(1-D)^2 + r_L + Dr_{sw} + \left(\frac{1}{2}\right)(1-D)^2 R^2 C_{SW} fs} \quad (9)$$

$$EFFICIENCY = \frac{Po}{Po + P_{Loss}} \quad (10)$$

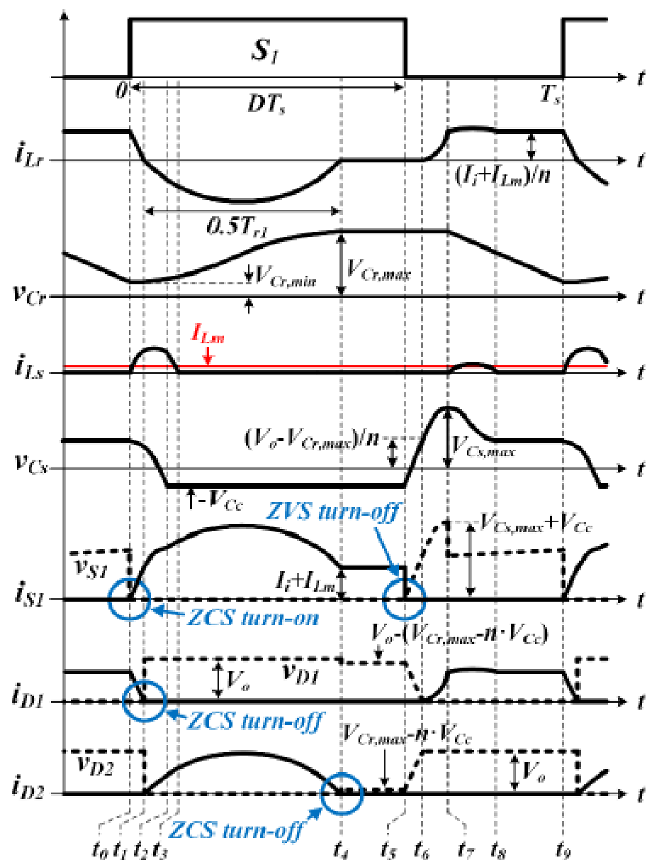

Fig .4 Effects of soft switching using ZVS & ZCS

Fig.3 shows the circuit diagram of isolated boost converter. It consist of input filter inductor Li , switch S1 a lossless snubber which includes capacitor Cs, inductor Ls, and diodes Ds1and Ds2, and clamp capacitor Cc at the primary side and Lr-Cr series resonant circuit and diodes D1and D2 at the secondary side. The lossless snubber achieves ZVS turn- off of switch. the voltage spikes of the switch by leakage inductance. Also, the Lr- Crseries resonant circuit makes it possible to achieve ZCS turn-off of diodes.

$$f_{r1} = \frac{1}{T_{r1}} = \frac{1}{2\pi\sqrt{L_r C_r}} \quad (11)$$

The total switching losses are smaller for below resonance operation resonance operation (DTs> 0.5Tr1). Since both turn-off current and diode di/dt of the below- resonance operation are smaller than above resonance operation. Therefore, the below resonance operation is selected for isolated boost converter operation. *A. Operating Principle*

Fig.3 shows waveforms of the proposed converter in the below-resonance operation. In order to simplify the analysis of the steady-state operation, it is assumed that the input filter and magnetizing inductances are large enough so that they can be treated as constant current sources during a switching period. It is also assumed that clamp and output capacitances are large enough so that they can be treated as constant voltage sources during a switching period. The voltage VCc across the clamp capacitor is the same as the input voltage Vi. In the below-resonance operation, nine modes exist within Ts.

Mode 1 (t0-t1): This mode starts when switch S1 is turned ON. Ls and Cs start resonating and resonant current *iLs* flows through *Ls*, *Ds1*, *Cs*, and *S1*. The voltage and current of resonant components are determined, as follows,

$$i_{Ls}(t) = v_{Cs}(t_0)\sqrt{\frac{C_s}{L_s}}\sin(\omega_{r2}(t-t_0)), \quad t_0 < t < t_2$$

$$v_{Cs}(t) = v_{Cs}(t_0)\cos(\omega_{r2}(t-t_0)), \quad t_0 < t < t_2$$

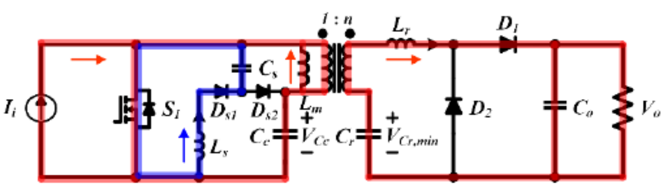

Fig. 5. Mode 1

*Mode 2 (t1-t2):*This mode started with current iLr. When it changes its direction L*r* and C*r* start resonating and resonant current iLr flows through Lr, Cr, and D2.

Mode 3 (t2-t3): In this mode is turned ON. Current *iLs* is determined by following equation, and this mode ends when current *iLs* reaches 0A.

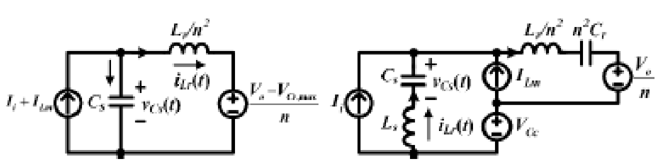

Fig. 6. Equivalent resonant circuits: (a) Mode 1-2 (t0-t2). (b) Mode 2-4 (t1-t4). (c) Mode 7 (t6-t7). (d) Mode 8 (t7-t8).

Mode 4 (t3-t4): The Lr-Cr resonance keeps on during this mode and ends when current iLr reaches 0A. Note that diode D2 *is* turned OFF under ZCS condition.

Mode 5 (t4-t5): In this mode a constant current flows through S1 whose value is the sum of the input current Ii and the magnetizing current ILm.

Mode 6 (t5-t6): This mode started with S1 is turned OFF. Then, Ii + ILm flows through *Cs*, *Ds2*, and *Cc*. Voltage across snubber capacitor *Cs* which is determined by the following equation increases linearly with the slope of *(Ii+ILm)*/*Cs*, resulting in ZVS turn-off of *S1*.

Mode 7 (t6-t7): D1 is turned ON at this mode. Equivalent circuit of this mode is shown in Fig. 6(c). Lr and Cs start resonating and resonant current *iLr* flows through *Cs*, *Ds2*, *Lr*, *D1*, and *Cr*. Assuming that *Cs* << *n2Cr*, *vCr* can be considered constant, and resonance frequency can be determined by *Cs* and *Lr*.

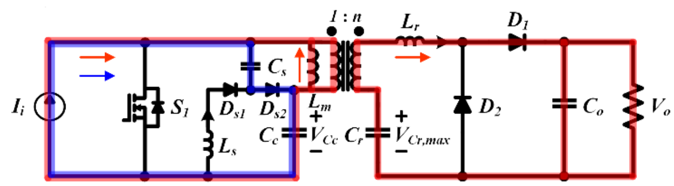

Fig. 7. Mode 7

B. Closed Loop Isolated Boost Converter with Single Switch

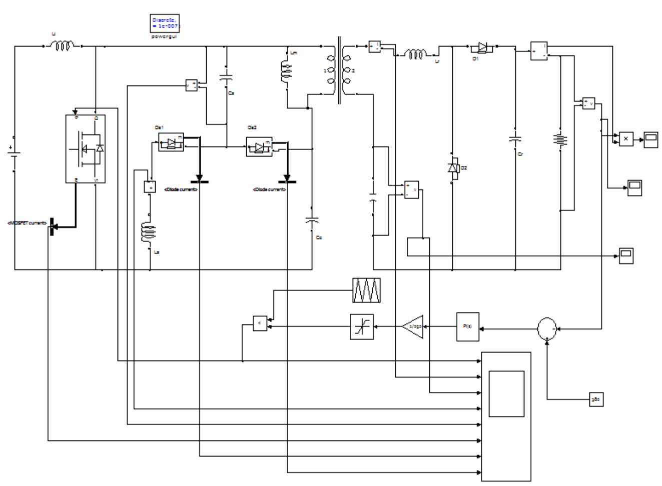

Fig. 8. Closed loop operation of isolated boost converter

C. Design Procedure

1) Determination of voltage gain:

Let us take,

ILs,avg = 0.27A

For below resonance operation,

$$\frac{V_o}{V_i} \approx \frac{n}{1-D} \quad (13)$$

$$D = \pi f_s \sqrt{L_r C_r} \quad (14)$$

$$t_1 - t_0 = \frac{(I_i - I_{Lm})L_r}{nVo\left(1 + \frac{1}{2CrfsRo}\right)} \quad (15)$$

The transformer n is chosen to be 5,

Resonant values of Lr and Cr are determined by 5μH and 560nF.

$$Vcs = \frac{Ii + ILm}{n}\sqrt{\frac{Lr}{Cs}} + \frac{Vo - Vcr}{n} \quad (16)$$

From the above equation the snubber capacitance Cs determined as 16 nF.

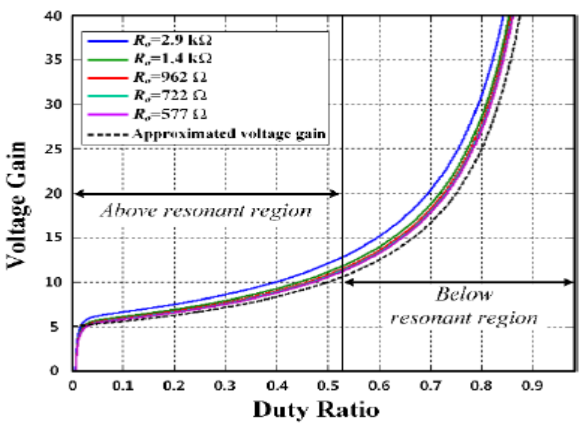

Fig. 9. Voltage gain of the proposed converter (Vi = 28V, Lr = 5ìH, Cr = 560nF, Ls = 5ìH, Cs = 16nF, n = 5, fs = 100kHz).

Dc input voltage	V_S = 28 V
Dc output voltage	V_O = 380 V
Switching Frequency	f_s = 100 KHz
Output Power	P_o = 250 W
Resonant Inductor(L_r)	Lr = 5 μH
Resonant Capacitor(C_r)	Cr= 560μF
Output resistance(R_o)	Ro = 577 Ω
Filter inductance	Li = 100 μH
Turns ratio of transformer	1:5
Power switching	IRFP4568
Power Diode	MBR1045
Snubber inductance(L_s)	5 μH
Snubber Capacitor(C_S)	16nF

TABLE I Components Rating and Selected Devices

3. EXPERIMENTAL RESULTS

A 250W laboratory prototype of the proposed converter has been built and tested to verify the proposed concept. Component ratings and selected devices of the proposed converter are listed in Table I.

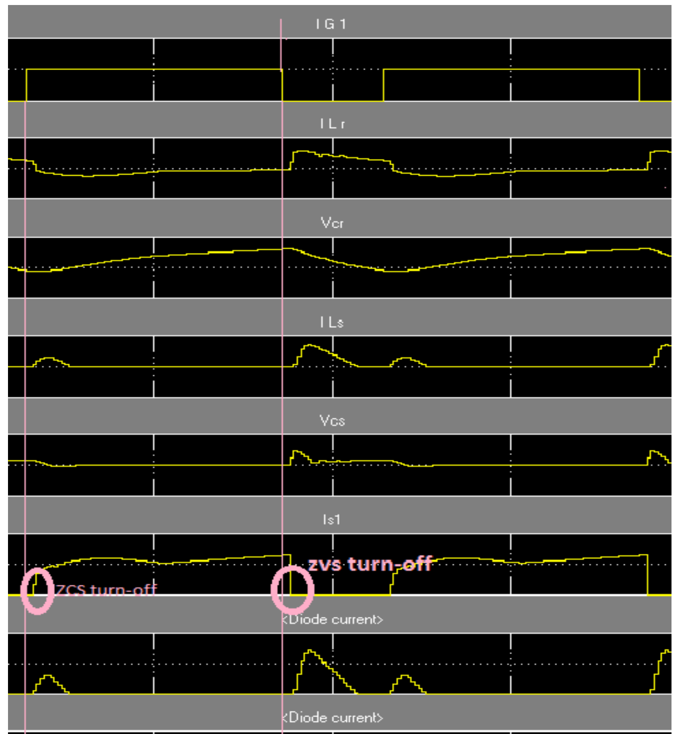

Fig. 10.Experimental waveforms at Vi =28v, Ro = 577Ω.

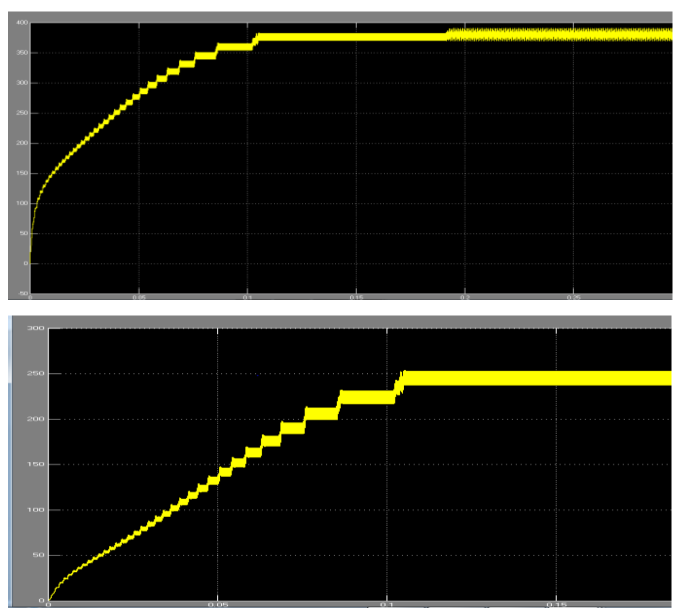

Fig. 11. Waveforms under closed loop conditions.(a) output power Po=250w, (b) output voltage Vo=380v

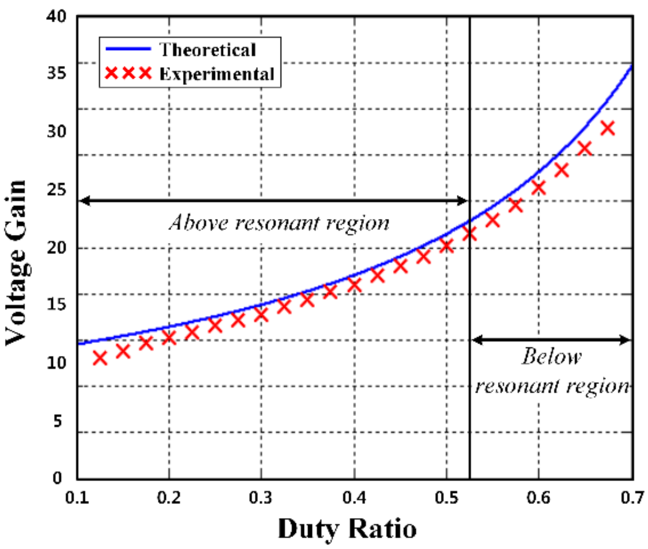

Fig. 12. Theoretical and experimental voltage gain of the proposed converter under Vi = 28V, Ro = 577Ω.

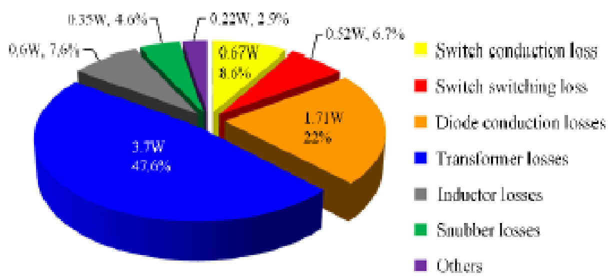

Fig. 13. Loss analysis of the proposed converter at full load (Vi= 38V).

4. CONCLUSION

This soft switched converter propsed for step-up application. Here we used single switch and diode low rater lossless snubber circuit achieves low cost and high power density compared to conventional flyback converter. Experimental results on a 100kHz, 250W prototype are provided to validate the proposed concept.The maximummeasured efficiency of 97.0% was obtained at full load.

REFERENCES

[1] B.R. Lin, B.R. Hou, ―Analysis of a zero voltage switching DC/DC converter without output inductor,‖ IET Trans. Power Electron., vol. 5, no. 6, 790 – 800, July 2012.
[2] Y. Tsuruta, Y. Ito, and A. Kawamura, ―Snubber-assisted zero- voltage and zero-current transition bilateral buck and boost chopper for EV drive application and test evaluation at 25kW,‖ IEEE Trans. Ind. Electron., vol. 56, no. 1, pp. 4–11, Jan. 2009.
[3] Y.M. Liu and L.K. Chang, ―Single-stage soft-switching ac–dc converter with input-current shaping for universal line applications,‖ IEEE Trans. Ind. Electron., vol. 56, no. 2, pp. 467–479, Feb. 2009.
[4] P.Sreeja and Dr.L.Padma Suresh,‖ PWM Based Closed Loop Control of Soft Switched Non Isolated High Multiplying Factor DC-DC Boost Converters,‖3rd International Conference on Electronics, Biomedical Engineering and its Applications (ICEBEA'2013) April 29-30, 2013 Singapore.
[5] H. Mao, O. A. Rahman, and I. Batarseh, ―Zero-voltage- switching DC-DC converters with synchronous rectifiers,‖ IEEE Trans. Power Electron., vol. 23, no. 1, pp. 369–378, Jan. 2008.
[6] S.H. Park, S.R. Park, J.S. Yu, Y.C. Jung and C.Y. Won, ―Analysis and design of a soft switching boost converter with an HI-bridge auxiliary resonant circuit,‖ IEEE Trans. on Power Electronics, vol. 25, no. 8, pp. 2142-2149, August 2010.
[7] A. K. Rathore, A. K. S. Bhat, and R. Oruganti, ―Analysis, design, and experimental results of wide range ZVS active-clamped l-l type current-fed dc/dc converter for fuel cells to utility interface,‖ IEEE Trans. Ind. Electron., vol. 59, no. 1, pp. 473–485, Jan. 2012.
[8] Simon ang and Alejandro Oliva, power-switching converters, 2nd ed., published in 2005, Taylor & Francis group, 6000 broken sound parkway NW, Suite 300 Boca Raton, FL 33487-2742.
[9] Daniel W.Hart ,Power Electronics, Published by McGraw-Hill, a business unit of The McGraw-Hill Companies, Inc., 1221 Avenue of the Americas, New York, NY10020.
[10] Z. Zhao, M. Xu, Q. Chen, J.-S. Lai, and Y. Cho, ―Derivation, analysis, and implementation of a boost-buck converter-based high-efficiency PV inverter,‖ IEEE Trans. Power Electron., vol. 27, no. 3, pp. 1304–1313, Mar. 2012.
[11] A. Mousavi, P. Das, and G. Moschopoulos, ―A comparative study of a new ZCS dc-dc full-bridge boost converter with a ZVS active-clamp converter,‖ IEEE Trans. Power Electron., vol. 27, no. 3, pp. 1347–1358, Mar. 2012.